Chinese Journal of
POLYMER SCIENCE

REVIEW

https://doi.org/10.1007/s10118-023-2944-0
Chinese J. Polym. Sci. **2023**, *41*, 640–651

Recent Research Progress of *n*-Type Conjugated Polymer Acceptors and All-Polymer Solar Cells

Xiao-Jun Li[a*], Guang-Pei Sun[a,b], Yu-Fei Gong[a,b], and Yong-Fang Li[a,b,c*]

[a] *Beijing National Laboratory for Molecular Sciences, CAS Key Laboratory of Organic Solids, Institute of Chemistry, Chinese Academy of Sciences, Beijing 100190, China*
[b] *School of Chemical Science, University of Chinese Academy of Sciences, Beijing 100049, China*
[c] *Laboratory of Advanced Optoelectronic Materials, Suzhou Key Laboratory of Novel Semiconductor Materials and Devices, College of Chemistry, Chemical Engineering and Materials Science, Soochow University, Suzhou 215123, China*

Abstract The active layer of all polymer solar cells (all-PSCs) is composed of a blend of a *p*-type conjugated polymer (*p*-CP) as donor and an *n*-type conjugated polymer (*n*-CP) as acceptor. All-PSCs possess the advantages of light weight, thin active layer, mechanical flexibility, low cost solution processing and high stability, but the power conversion efficiency (PCE) of the all-PSCs was limited by the poor photovoltaic performance of the *n*-CP acceptors before 2016. Since the report of the strategy of polymerized small molecule acceptors (PSMAs) in 2017, the photovoltaic performance of the PSMA-based *n*-CPs improved rapidly, benefitted from the development of the A-DA′D-A type small molecule acceptors (SMAs). PCE of the all-PSCs based on the PSMA acceptors reached 17%–18% recently. In this review article, we will introduce the development history of the *n*-CPs, especially the recent research progress of the PSMAs. Particularly, the structure-property relationship of the PSMAs is introduced and discussed. Finally, current challenges and prospects of the *n*-CP acceptors are analyzed and discussed.

Keywords *n*-Type conjugated polymers; All-polymer solar cells; Polymer acceptors; Polymerized small molecule acceptors

Citation: Li, X. J.; Sun, G. P.; Gong, Y. F.; Li, Y. F. Recent research progress of *n*-type conjugated polymer acceptors and all-polymer solar cells. *Chinese J. Polym. Sci.* **2023**, *41*, 640–651.

INTRODUCTION

Polymer solar cells (PSCs) have attracted great attention in recent years, owing to their advantages of light weight, thin and flexible active layer, and low cost solution-processing.[1–5] Photovoltaic active layer of the PSCs is composed of a blend of a *p*-type conjugated polymer (*p*-CP) as donor and an *n*-type organic semiconductor (*n*-type conjugated organic small molecule or *n*-type conjugated polymer (*n*-CP)) as acceptor.[4] If the active layer is the blend of a *p*-CP as donor and an *n*-CP as acceptor, the device is called as all-polymer solar cell (all-PSCs). In addition to the advantages of the common PSCs, all-PSCs possess additional advantages of good film-forming property,[6] high morphology stability and excellent mechanical flexibility, which is very important for roll-to-roll fabrication and future application of the flexible PSCs.

In 1995, Heeger *et al*. reported the first solution-processed PSCs with a bulk-heterojunction (BHJ) blend active layer of a *p*-type conjugated polymer MEH-PPV as donor and soluble C_{60} derivative PCBM as acceptor.[7] And in the same year, they also reported all-PSCs based on *p*-CP MEH-PPV as donor and *n*-CP CN-PPV as acceptor.[8] However, until the year of 2017, PCE of the all-PSCs was much lower than that of the PSCs based on fullerene derivative[9] or narrow bandgap small molecule acceptor[10] as acceptors, due to the lack of high performance polymer acceptors. At early stage, the polymer acceptors used in the all-PSCs were mainly the D-A copolymers based on the A-unit of perylene diimide (PDI) or naphthalene diimide (NDI).[11,12] The weak absorbance in long wavelength range and poor aggregation property of the polymer acceptors resulted in low short circuit current density (J_{sc}) and lower fill factor (FF), so that lead to low PCE of the all-PSCs. In 2017, in considering the strong absorbance in the long wavelength region and suitable aggregation property of the narrow bandgap small molecule acceptors (SMAs),[13,14] Zhang *et al*. proposed the concept of polymerizing small molecule acceptor to synthesize the polymer acceptors.[15] The polymerized small molecule acceptors (PSMAs) preserved the advantages of strong absorption, suitable electronic energy levels and appropriate aggregation for the SMAs.[16] Therefore, PCE of the all-PSCs based the PSMA polymer acceptors has rapidly increased to over 17% recently.[17,18]

In the following, we will introduce the development history, molecular structures, physicochemical and photovoltaic properties of the *n*-type conjugated polymer acceptors (especially the PSMAs), in more details.

* Corresponding authors, E-mail: lixiaojun@iccas.ac.cn (X.J.L.)
E-mail: liyf@iccas.ac.cn (Y.F.L.)

Special Issue: In Memory of Professor Fosong Wang
Received December 11, 2022; Accepted December 31, 2022; Published online February 27, 2023

DEVELOPMENT HISTORY OF THE *N*-TYPE CONJUGATED POLYMER ACCEPTORS AND ALL-PSCS

The first all-PSCs reported in 1995 with *n*-CP CN-PPV (Fig. 1) as acceptor, showed a low PCE of *ca*. 0.2%.[8] In 2007, Zhan *et al*. developed an *n*-type D-A copolymers PDI-DTT (Fig. 1) based on PDI A-unit, and the PDI-DTT-based all-PSC with a polythiophene derivative with conjugated side chains as donor displayed a PCE of *ca*. 1%.[19] Then a series of the PDI- and NDI-based D-A copolymers were synthesized and reported for the application as polymer acceptors in the all-PSCs,[11,12] among them the NDI-based D-A copolymer N2200 (Fig. 1) is a representative polymer acceptor.[20,21] Benefitted from the development of polymer donors and optimization of the morphology of the active layer, the PCE of the N2200-based all-PSCs increased to over 5% at the end of 2015.[22] In 2016, a medium-band-gap polymer J51[23] was used as the donor, which is absorption-complementary with N2200 in the visible-near infrared region, promoting the PCE of the N2200-based all-PSCs to 8.27%.[24] In 2019, the PCE of the N2200-based all-PSCs reached over 11.50% with the polymer PTzBI-Si as the donor.[25] In addition to the NDI/PDI-based D-A copolymer acceptors, other D-A copolymer acceptors have also been explored, based on the A-units of diketopyrrolopyrrole,[26] bithiophene imides[27] and B-N bridged unit,[28,29] *etc*., but PCEs of the related all-PSCs are limited to lower than 10%.

Further development of all-PSCs is limited by weak points of the D-A copolymer acceptors, such as their weak absorbance in the long wavelength region and poor morphology of their blend active layers with polymer donor. Fortunately, the narrow-bandgap SMAs were developed in 2015,[13] and SMAs possess the advantages of narrow energy bandgap, strong absorption coefficient and appropriate aggregation property. Consideration of the advantages of the SMAs, Zhang *et al*. proposed a strategy of polymerizing small-molecule acceptor in 2017, and synthesized a polymer acceptor PZ1 (see Fig. 1) based on SMA IDIC as the main building block copolymerized with a thiophene linking unit.[15] The all-PSCs with PZ1 as polymer acceptor and PBDB-T as polymer donor demonstrated a higher PCE of 9.19%, which is the highest efficiency of the all-PSCs in 2017. By using PM6 as polymer donor, PCE of the PZ1-based all-PSC was promoted to 11.2% (entry 1 in Table 1).[30] The PSMA strategy combined the advantages of the SMAs with strong absorption in NIR region, suitable electronic energy levels and appropriate aggregation, and the advantages of the polymers with good flexibility and the higher morphology stability.[16] Therefore, the PSMA polymer acceptors and the PSMA-based all-PSCs have attracted great attention in recent years. In the following, we will introduce the research progress of the PSMAs, including the studies on the effect of SMA building blocks and linkage units on the physicochemical and photovoltaic properties of the PSMAs and the ternary and tandem all-PSCs.

EFFECT OF THE SMA BUILDING BLOCKS ON THE PHOTOVOLTAIC PERFORMANCE OF THE PSMAS

In the synthesis of the first PSMA PZ1, the SMA building block is IDIC-C16 which possesses longer side chains in comparison with the SMA IDIC for improving solubility of the PSMA. In comparison with the absorption spectrum of IDIC-C16 film, the absorption spectrum of PZ1 film is red-shifted by *ca*. 50 nm, showing an absorption edge at 800 nm with a narrow band gap of 1.55 eV.[15] These results indicate the advantage of the PSMA strategy in broadening the absorption for better light harvesting of the corresponding all-PSCs.

The SMA building blocks are the most important part of the PMSAs, and the strategies reported in literatures to tune the opto-electronic properties of the SMAs are also applicable to the PMSAs. Comparing to PZ1, PT-IDTTIC (Fig. 2) with the ITIC-like SMA as the main building block further extended the absorption and decreased the band gap to 1.49 eV, and the PT-IDTTIC-based all-PSC realized a higher PCE of 11.69% with a higher J_{sc} of 17.9 mA·cm^{-2} (entry 2 in Table 1).[31] To take the advantage of the Y6-type SMAs with strong absorption in the NIR region and excellent photovoltaic performance, several groups synthesized the PSMAs with Y6-type SMAs[32] as the building block, such as PJ1[33] and series of PYT[34] (Fig. 2), *etc*. These PSMAs preserve all the merits of their corresponding Y6 derivative SMA segment and show strong absorption in the wavelength range of 600–900 nm. The all-PSC based on the PSMAs achieved the significantly improved PCE of over 14% with a higher J_{sc} over 21 mA·cm^{-2} (entries 3 and 4 in Table 1). Compared with IDIC and ITIC-type PSMAs, the Y6 derivative-based PSMAs possess narrower bandgap, the wider absorption and stronger intermolecular interaction, which results in higher J_{sc} and higher FF for their corresponding all-PSCs.

Compared to the conventional thiophene units in the DA′D fused ring of the PSMAs, the PSMAs with selenophene-containing DA′D fused ring typically have a further reduced optical band gap, which affords enhanced J_{sc} than their thiophene-based counterparts in the all-PSCs. On the basis of the advantage of selenophene, Fan *et al*. prepared the multi-selen-

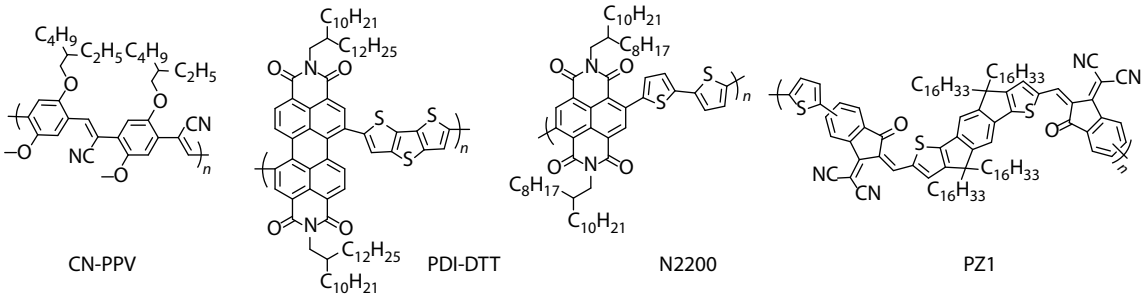

Fig. 1 Molecular structures of typical polymer acceptors.

https://doi.org/10.1007/s10118-023-2944-0

Table 1 Photoactive layer compositions and photovoltaic parameters of binary all-PSCs.

Entry	Acceptor	Donor	V_{oc} (V)	J_{sc} (mA·cm^{-2})	FF	PCE (%)	Ref.
1	PZ1	PM6	0.96	17.1	0.68	11.2	[30]
2	PT-IDTTIC	PM6	0.97	18.0	0.67	11.7	[31]
3	PJ1	PBDB-T	0.90	22.3	0.70	14.4	[33]
4	PYT	PM6	0.93	21.8	0.66	13.4	[34]
5	PYF-3Se	PBDB-T	0.87	23.6	0.74	15.1	[35]
6	PZT	PBDB-T	0.91	23.2	0.69	14.5	[37]
7	PS-Se	PBDB-T	0.87	23.3	0.68	13.8	[38]
8	PN-Se	PBDB-T	0.91	24.8	0.72	16.2	[38]
9	PY-DT	PM6	0.95	23.7	0.74	16.8	[39]
10	PY-IT	PM6	0.93	22.3	0.72	15.1	[40]
11	PY-IOT	PM6	0.94	19.7	0.66	12.1	[40]
12	PFA1	PTzBI-oF	0.87	24.0	0.73	15.1	[41]
13	PY2F-T	PM6	0.86	24.3	0.73	15.2	[42]
14	PIDIC2T	PM6	0.90	10.5	0.52	4.9	[43]
15	PIDIC2T2Cl	PM6	0.90	12.7	0.62	7.1	[43]
16	PBTIC-γ-2F2T	PM6	0.95	22.6	0.67	14.3	[44]
17	PBTIC-γ-2T	PM6	0.95	20.9	0.60	11.9	[44]
18	PY-V-γ	PM6	0.91	24.8	0.76	17.1	[45]
19	PFBDT-IDTIC	PM6	0.96	15.3	0.68	10.3	[47]
20	PF5-Y5	PBDB-T	0.95	20.7	0.74	14.5	[48]
21	L14	PM6	0.96	20.6	0.72	14.3	[49]
22	PY5-BTZ	PBDB-T	0.92	22.6	0.71	14.8	[50]
23	PYF-2TS	PBDB-T	0.91	20.5	0.66	12.3	[51]
24	PY-IT2F	PM6	0.91	22.2	0.70	14.1	[17]
25	PG-IT2F	PM6	0.95	24.0	0.76	17.2	[17]
26	QM1	PM6	0.91	25.2	0.74	17.1	[52]

ophene-containing PSMA PFY-3Se (Fig. 2),[35] which shows an obviously red-shifted absorption spectrum, increased electron mobility, and improved intermolecular packing in films compared to its selenophene-free analog PFY-0Se (also named PYT). As a result, the all-PSC with PFY-3Se as polymer acceptor yields a PCE of 15.1% with a high J_{sc} of 23.6 mA·cm^{-2} (entry 5 in Table 1). Jen *et al*. also synthesized a PSMA with an asymmetrical selenophene-fused backbone, and the PSMA demonstrated a higher photovoltaic performance with PCE of 16.3% for its corresponding all-PSCs.[36]

The A′ unit in the DA′D fused ring also influence the photovoltaic performance of the PSMAs, just like its influence on the A-DA′D-A SMAs. In comparison with the A′ unit of benzothiadiazole (BT), benzotriazole (BTz) with weaker electron withdrawing ability as A′ unit can broaden the absorption spectrum of the PSMA and can attach an alkyl side chains on the top nitrogen atom of BTz. Replacement of BT in the PSMA PYT with BTz affords the PSMA PZT (Fig. 2). Compared with PYT, PZT shows higher lying HOMO/LUMO energy levels and red-shifted absorption, which contribute to higher V_{oc} (0.909 V for the PZT-based device versus 0.892 V for the PYT-based device) and J_{sc} (23.2 mA·cm^{-2} for the PZT-based device versus 20.8 mA·cm^{-2} for the PYT-based device).[37] The all-PSCs based on PZT exhibit a higher PCE of 14.5% than that (12.9%) of the device based on PYT (entry 6 in Table 1). Du *et al*. synthesized two PSMAs of PS-Se (Fig. 2) with BT as A′ unit and PN-Se (Fig. 2) with BTz A′ unit, and with selenophene as linking unit. PN-Se shows more red-shifted absorption than PS-Se and suitable electronic energy levels for the application in the all-PSCs with PBDB-T as the polymer donor. A bicontinuous-interpenetrating network in the PBDB-T:PN-Se blend film with an aggregation size of 10–20 nm is observed by the photoinduced force microscopy. The desirable morphology of the PBDB-T:PN-Se active layer leads to its all-PSC showing a higher PCE of 16.16% (entries 7 and 8 in Table 1).[38]

Side chain engineering of the PSMAs also plays an important role on tuning their photovoltaic properties. In addition to improving solubility in organic solvents, the alkyl side chains can also regulate the intermolecular interaction of the PSMAs. For example, Sun *et al*. synthesized the PSMA PY-DT (Fig. 2) by changing the linear upper side chain of PYT to branched upper side chain, and the PCE of all-PSC based on PM6:PY-DT increased to 16.76% with the V_{oc} of 0.949 V, J_{sc} of 23.73 mA·cm^{-2} and FF of 74.4% (entry 9 in Table 1).[39] In contrast to PYT, the improved efficiency in the PY-DT-based device is mainly ascribed to its decreased energy loss, optimized phase separation, and suppressed non-radiative recombination.

In the SMAs, the halogen substituted end group is a mixture of two isomers, and the same is true for the brominated end group (IC-Br) used in the polymerization for the PSMAs. To exclude the effect of isomerization on device performance, Yang *et al*. separated IC-Br (in) and IC-Br (out) (where "in" and "out" indicate that the bromine and carbonyl groups are on the same side and the opposite side, respectively) and synthesized the regioregular polymers PY-IT (Fig. 2) and PY-OT (Fig. 2) by using an isomer-free reagent.[40] The PY-IT synthesized by using the IC-Br (in) displays a lower LUMO, a red-shifted and stronger absorption and higher electron mobility relative to the regiorandom PY-IOT (also named PYT). The devices based on PY-IT show an improved PCE of 15.05% in comparison with that of PY-IOT (12.12%), which is mainly ascribed to a more balanced charge transport, and favorable morphology (entries 10 and 11 in Table 1). Fluorination of end groups in the SMAs has been proven to be a successful

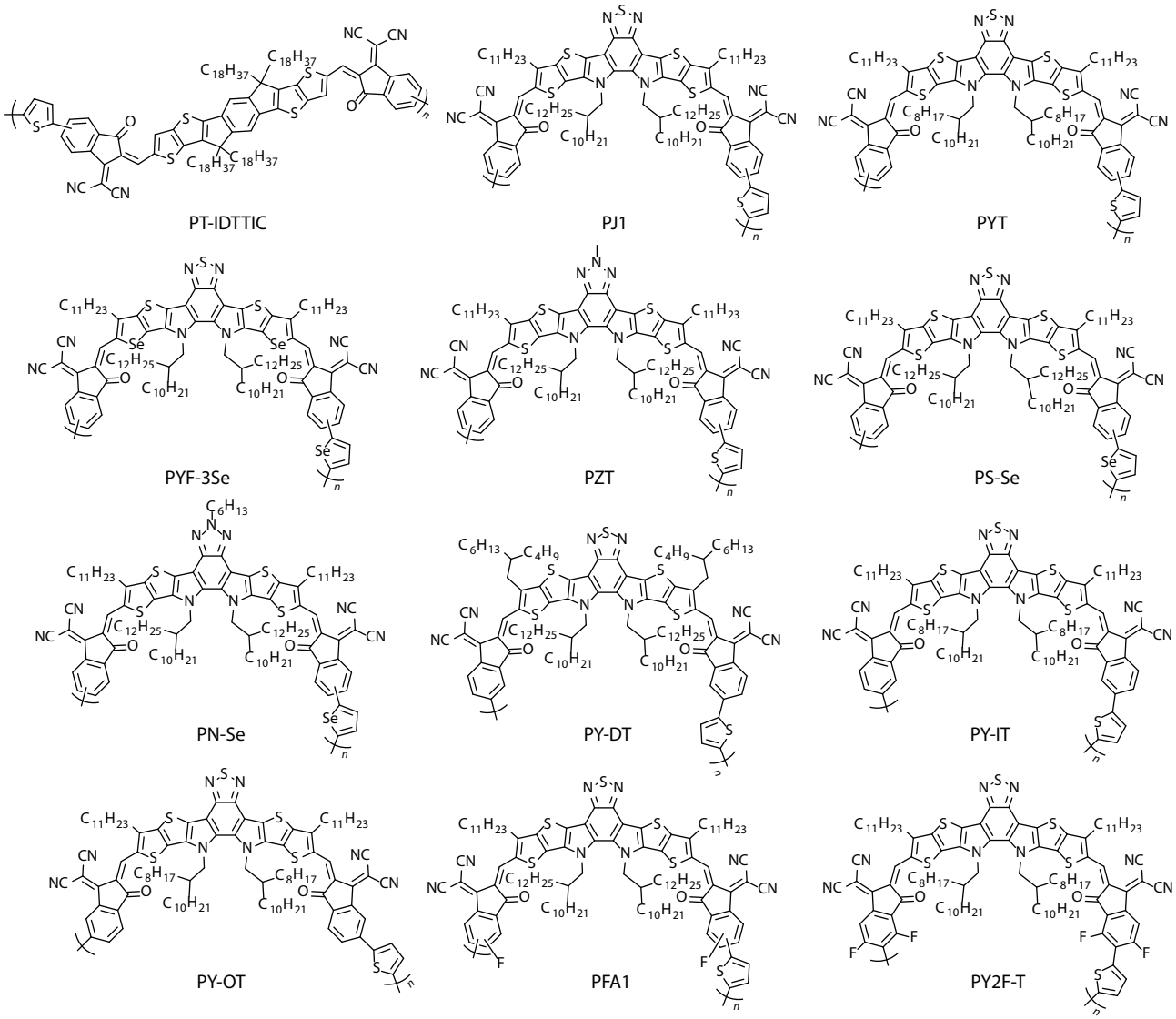

Fig. 2 Molecular structures of the PSMAs with different SMA building blocks and thiophene or selenophene linking units.

strategy for red-shifting absorption and enhancing the intermolecular interaction of the polymers. In considering the fluorination effect of the SMAs, Cao *et al*. synthesized a PSMA PFA1 (Fig. 2) based on the SMA with a fluorine-substituted end group.[41] Benefitted from the electron-withdrawing ability of fluorine, PFA1 shows red-shifted absorption and low-lying energy levels relative to the corresponding PYT without the fluorine substitution. When blended with PTzBI-oF polymer donor, due to the special fluorine supermolecular interaction, the PTzBI-oF:PFA1 active layer formed stronger intermolecular packing thus leading to a more effective exciton dissociation and lower extent of charge recombination. Consequently, the all-PSC based on PFA1 demonstrated a higher PCE of 15.11% with a higher J_{sc} and improved FF than that of the PYT-based device (entry 12 in Table 1). In addition, Min and Yan *et al*.[42] synthesized the PSMA PY2F-T (Fig. 2) based on the SMA with difluorine-substituted end group, and the PY2F-T-based all-PSC displayed a PCE of 15.22% (entry 13 in Table 1).

EFFECT OF LINKING UNITS ON THE PHOTOVOLTAIC PERFORMANCE OF THE PSMAS

Modifications on linking units can also affect the molecular orbital energy levels, absorption, active layer morphology and photovoltaic properties of the PMSA. Besides the thiophene linking unit used in the first PSMA PZ1, bithiophene (bT) was also used as the linking unit in the PSMAs. Yuan *et al*. synthesized the PSMAs of PIDIC2T, PIDIC2T2F, and PIDIC2T2Cl (Fig. 3) with IDIC-type SMA as building block and bT as linking unit.[43] The halogen substitution on the linking unit can significantly promote the intermolecular *π*-*π* stacking and thus increase electron mobility. The PIDIC2T2Cl based devices delivered a PCE of 7.11% relative to that (4.89%) of the PIDIC2T based device due to their favorable morphology and more balanced mobilities (entries 14 and 15 in Table 1). He *et al*. combined fluorinated bT linker and Y6-type SMA building block, and synthesized the PMSA PBTIC-*γ*-2F2T (Fig. 3).[44] Compared with its non-fluorinated analog PBTIC-*γ*-2T (Fig. 3) with PCE of

https://doi.org/10.1007/s10118-023-2944-0

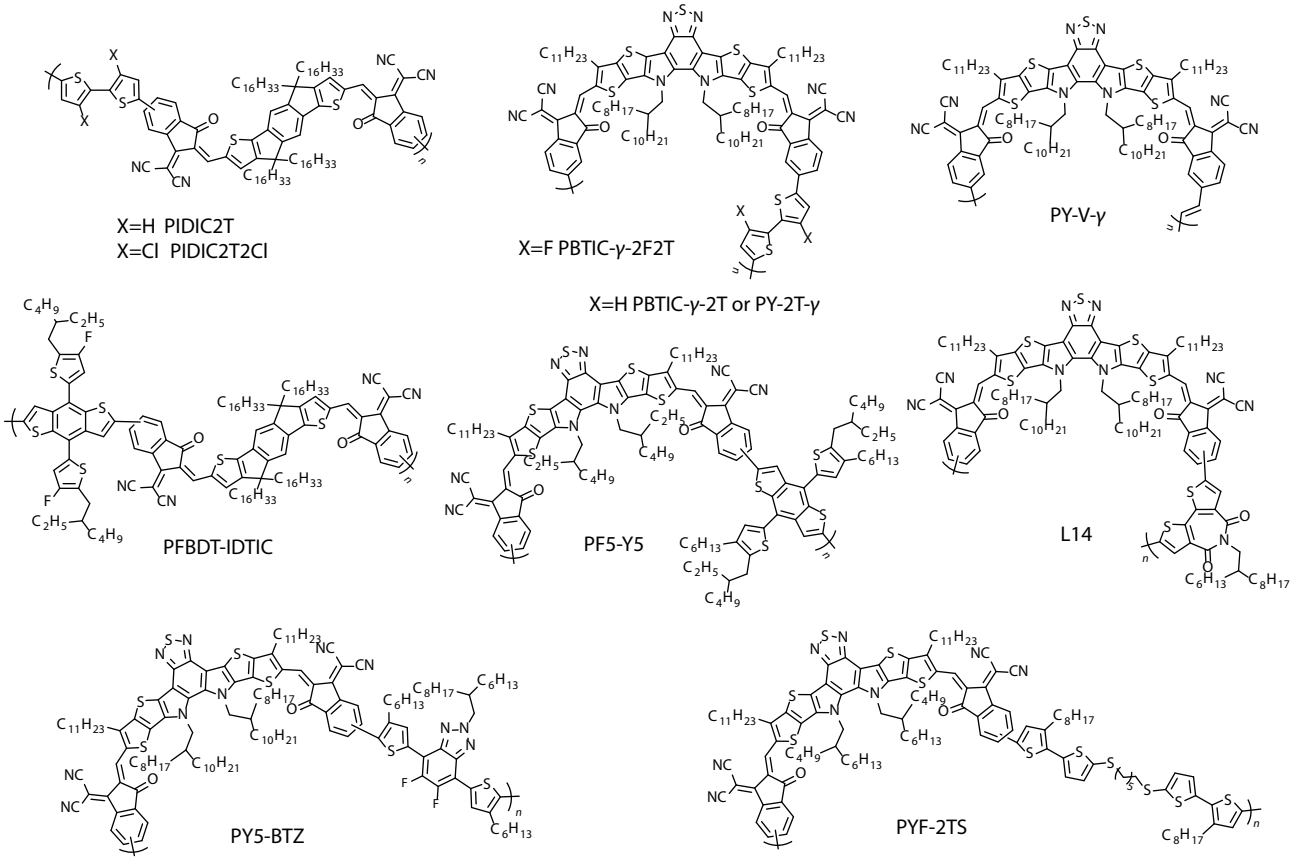

Fig. 3 Molecular structures of the PSMAs with different linking units.

11.92% for the PBTIC-γ-2T based device, PBTIC-γ-2F2T shows a red-shifted absorption and improved blend morphology, thus a favorable PCE of 14.34% was obtained for the PBTIC-γ-2F2T based all-PSC (entry 16 and 17 in Table 1). On the basis of PY-IT, Yan *et al*. also synthesized the PSMAs PY-V-γ (Fig. 3) and PY-2T-γ (Fig. 3) with vinylene or bT as linking units instead of the thiophene linking unit in PY-IT.[45] When blended with PM6 polymer donor, PY-V-γ polymer acceptor exhibits a denser interchain packing and more suitable phase separation. Meanwhile, the PY-V-γ-based device possessed decreased energy loss owing to the reduced energy disorder enabled by the vinylene-assisted rigid conformation.[46] Therefore, the all-PSCs based on PM6:PY-V-γ delivered a higher PCE of 17.1% with a higher J_{sc} of 24.75 mA·cm^{-2} and FF of 75.8% (entry 18 in Table 1), out-performing the PCE of 16.1% for the devices based on PM6:PY-IT.

Benzodithiophene (BDT) is a well-known electron-rich unit, which has been widely applied as the D-unit of D-A copolymer donors. Yan *et al*. designed a PMSA named PFBDT-IDTIC (Fig. 3) by replacing the thiophene linking unit in PZ1 with a fluorinated alkyl-thiophene-substituted BDT unit.[47] The film absorption edge of PFBDT-IDTIC is around 767 nm, which is slightly blue-shifted relative to that of PZ1 (800 nm). With PM6 as donor, the PFBDT-IDTIC-based all-PSCs displayed a PCE of 10.3% (entry 19 in Table 1). By introducing the BDT linking unit in the A-DA′D-A-type SMA based PSMAs, Fan *et al*. prepared the PSMA PF5-Y5 (Fig. 3).[48] Compared with PYT, the PSMA PF5-Y5 shows an up-shifted LUMO level (−3.84 eV for PF5-Y5 versus −3.92 eV for PYT), as a result, the PF5-Y5-based all-PSCs achieved a higher V_{oc} (0.95 V) than that of the PYT-based device with PBDB-T as polymer donor (entry 20 in Table 1).

Apart from the electron donating group, using electron-deficient linking units is another way to modify the photophysical properties of the PSMAs. Guo *et al*. synthesized the PSMA L14 (Fig. 3) by using electron-deficient distannylated bithiophene imide as linking units.[49] Relative to its thiophene-based counterparts, L14 shows a narrower energy bandgap and lower HOMO/LUMO levels. Owing to a smaller nonradiative recombination energy loss of 0.22 eV, the V_{oc} of L14-based device is as high as 0.95 V (entry 21 in Table 1). Other electron-withdrawing units were also used as linking unit in PMSAs. For example, Zhou *et al*. employed electron-withdrawing linking units of bifluorobenzotriazole, thiazolo[5,4-*d*]thiazole, pyrazine, and benzothiadiazole, and synthesized a series of PMSAs by copolymerizing them with a Y5-like SMA like PY5-BTZ (Fig. 3).[50] These PMSAs exhibit similar absorption spectra but diversified energy levels, the PY5-BTZ based device exhibits a PCE of 14.8% (entry 22 in Table 1).

Notably, besides conjugated linkages, the non-conjugated spacer can also as the linking unit to synthesize the PSMAs, such as PYF-2TS (Fig. 3).[51] Compared with conjugated PMSAs, the PSMAs with non-conjugated linking unit show similar optical absorption, but different molecular crystallinity. The non-conjugated linking units can favor a flexible backbone to avoid over aggregation of the blend active layer, and realize a

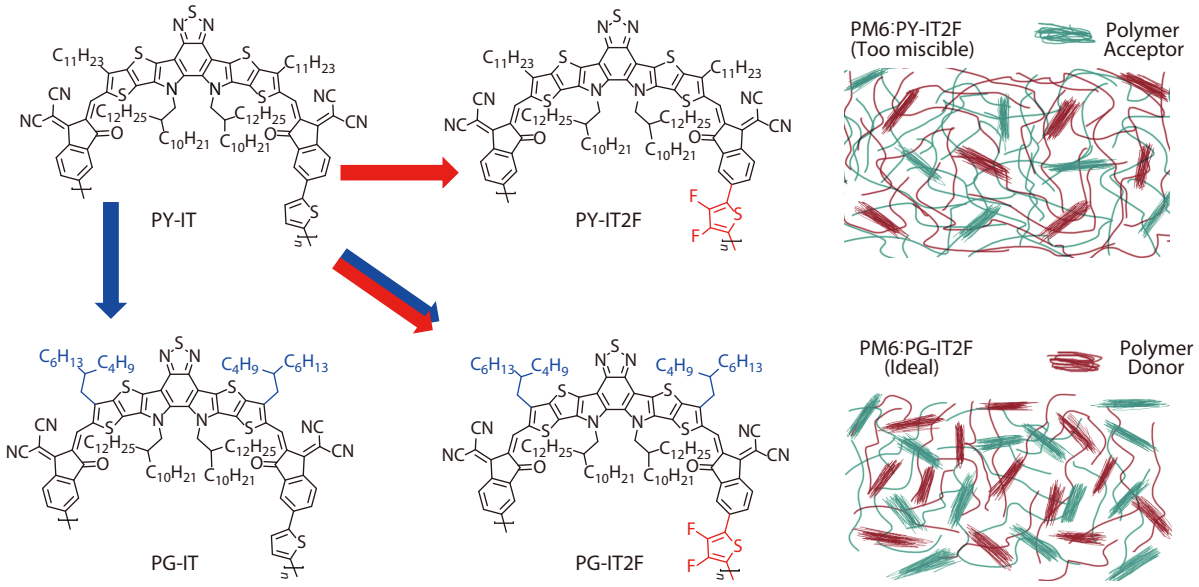

Fig. 4 Molecular structures of PY-IT, PY-IT2F, PG-IT, PG-IT2F and the schematic diagram of the morphology of PM6:PY-IT2F and PM6:PG-IT2F blend film.

promising PCE (entry 23 in Table 1) for its corresponding all-PSCs along with good thermal stability.

As mentioned above, both modifications of SMA building blocks and linking units can regulate the photovoltaic performance of the PSMAs. Recently, Sun *et al*. proposed a synergistic strategy of fluorinated thiophene π-bridge linker and branched alkyl upper side chain modification of the SMA building block, and synthesized a PSMA PG-IT2F (Fig. 4).[17] The introduction of fluorine atoms in π-bridges (PY-IT2F) can increase electron mobility than those of the non-fluorinated PSMA (PY-IT), which affords a more balanced charge carrier transport with longer charge carrier lifetime in the active layer. However, it will lead to excessive miscibility of acceptors with PM6 donor, resulting in poor photovoltaic performance. By attaching the branched alkyl upper side chains, PG-IT2F affords optimal miscibility with PM6 and the PM6:PG-IT2F blend active layer showed good morphology with nanoscaled interpenetrating networks. Therefore, the all-PSCs based on PM6:PG-IT2F displayed efficient exciton dissociation and decreased charge recombination, thus demonstrating a high PCE of 17.24% with higher J_{sc} and FF (entries 24 and 25 in Table 1). This work confirms the importance of synergistic regulation in improving the photovoltaic performance of the PSMAs.

In addition to the PSMAs mentioned above, recently Zou *et al*. synthesized an A-π-A structured organic acceptor QM1 by linking two SMA units with a thiophene π-bridge.[52] QM1 exhibits a special spiral-like molecular structure while retain favorable miscibility with the polymer donor PM6, and the QM1-based PSCs with PM6 as polymer donor displayed a higher PCE of 17.06% (entry 26 in Table 1).

TERNARY AND TANDEM ALL-PSCS

In the binary blend of polymer donor and polymer acceptor, it is challenging to achieve favorable donor/accepter contact and obtain suitable phase separation while maintain high molecular order in the blend films. To address this issue, the incorporation of a third component into binary polymer blend is considered to be an effective strategy. As early as 2015, Ito *et al*. reported a ternary all-PSC based on PBDTTT-EF-T:PCDTBT:N2200. As the third component, the addition of PCDTBT effectively promotes the increase of J_{sc}, and finally obtaining a PCE of 6.65%.[53] Since 2016, many research groups have made a lot of efforts in the construction of ternary all-PSC systems, and the efficiency of ternary all-PSCs increased rapidly in recent years.[54–64] For ternary all-PSCs, the third component can be either a polymer donor or a polymer acceptor, based on that, we divided ternary all-PSCs into donor 1:donor 2: acceptor (D1:D2:A) system and donor:acceptor 1:acceptor 2 (D:A1:A2) system.

For the D1:D2:A system, in 2020, Peng *et al*. synthesized the polymer donor PNDT-T based on the PBDB-T, and PNDT-T can be well matched with the polymer acceptor DCNBT-IDT (Fig. 5).[65] By adopting the *p*-doping agent F4-TCNQ and adding the second polymer donor PBDB-T to the PNDT-T:DCNBT-IDT system), the PCE is increased from 9.57% for the binary device based on PNDT-T:DCNBT-IDT to 11.87% for the ternary device (entry 1 in Table 2). In 2021 Li *et al*. fabricated high-efficiency ternary all-PSCs based on PBDB-T:PTPBT-ET$_{0.1}$ (Fig. 5) system and using low cost polymer donor PTQ10 as the third component.[66] Compared with the binary PBDB-T:PTPBT-ET$_{0.1}$ all-PSC, the ternary all-PSC showed an improved J_{sc} which should be attributed to the complementary absorption spectra and good compatibility of PBDB-T and PTQ10. In addition, the lower HOMO energy level of PTQ10 helps the ternary all-PSC to achieve higher V_{oc}, thus an optimal PCE of 14.56% was obtained (entry 2 in Table 2). After that, PTQ10 was further applied into PM6:PY-IT system as the third component to finely tune the energy-level matching and microscopic morphology of the active layer. As a result, a PCE of 16.52% was achieved for the ternary all-PSCs (entry 3 in Table 2). In addition, owing to the increased π-π stacking coherence length in blend films, photovoltaic performance of the ternary devices

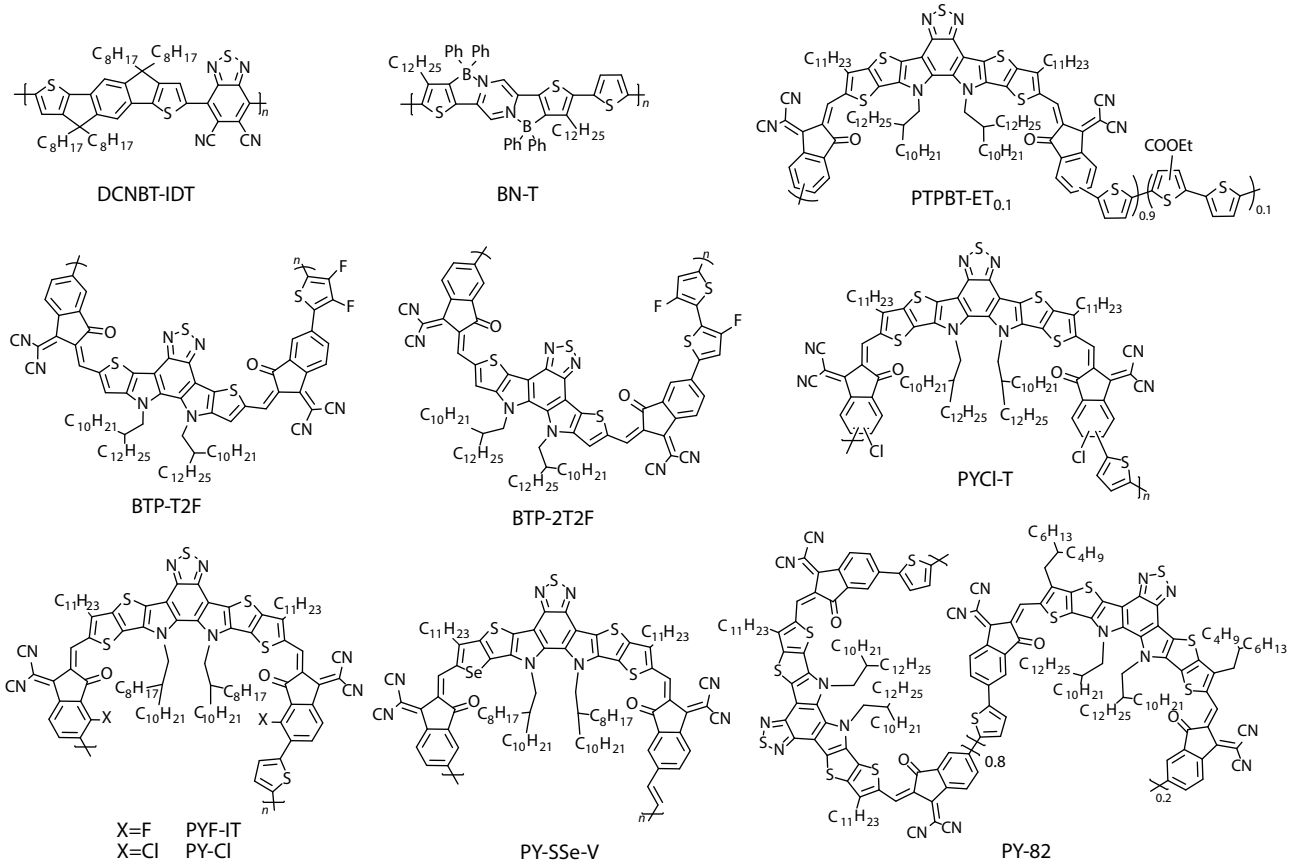

Fig. 5 Molecular structures of the PSMAs used in ternary all-PSC.

Table 2 Photoactive layer compositions and photovoltaic parameters of ternary and tandem all-PSCs.

Entry	Acceptor	Donor	Third component	V_{oc} (V)	J_{sc} (mA·cm^{-2})	FF	PCE (%)	Ref.
1	DCNBT-IDT	PNDT-T	PBDB-T	0.91	17.5	0.74	11.9	[65]
2	PTPBT-ET$_{0.1}$	PBDB-T	PTQ10	0.91	23.7	0.68	14.6	[66]
3	PY-IT	PM6	PTQ10	0.94	23.8	0.23	16.5	[67]
4	PFA1	PTzBI-oF	PM6	0.88	24.4	0.76	16.3	[68]
5	PY-IT	PM6	J71	0.94	23.3	0.75	16.5	[69]
6	BTP-2T2F	PTQ10	PBDTCl-TPD	0.89	23.9	0.75	16.0	[70]
7	PY-IT	PM6	BN-T	0.96	22.7	0.74	16.1	[71]
8	PY2F-T	PM6	PYT	0.90	25.2	0.76	17.2	[72]
9	PY-IT	PM6	PYCl-T	0.92	24.6	0.73	16.6	[73]
10	PY-IT	PM6	PYF-IT	0.92	24.1	0.75	16.6	[74]
11	PY-SSe-V	PM6	PY-Cl	0.91	25.9	0.77	18.1	[75]
12	PY-82	PM6	PY-DT	0.95	24.3	0.78	18.0	[76]
13	N2200 [a] P(NDI2HD-T) [b]	PBFSF [a] PTP8 [b]	\	1.77	8.00	0.59	8.3	[78]
14	N2200 [a,b]	PTzBI-Si [a,b]	\	1.72	08.9	0.72	11.2	[79]
15	PY-IT [a] PIDT [b]	PM6 [a] PM7 [b]	\	2.00	11.7	0.76	17.9	[80]

[a] Rear cell photovoltaic materials; [b] Front cell photovoltaic materials.

exhibited a high tolerance of the active layer thickness.[67] Cao *et al*. reported an efficient ternary all-PSC by replacing a certain amount of polymer donor PTzBI-oF with the counterpart polymer PM6 when blending with the PSMA PFA1 (Fig. 2). Compared with binary all-PSC based on PTzBI-oF:PFA1 with a PCE of 14.8%, the incorporation of PM6 resulted in Förster resonance energy transfer with PTzBI-oF, reduced non-radiative recombination energy loss, and led to optimal film morphology, which leads to an improved PCE of 16.3% (entry 4 in Table 2).[68] Besides of PTQ10, J71 is also frequently used as the third component in the PM6-based all-PSCs due to its good miscibility with PM6. Gao *et al*. reported a ternary all-PSCs based on PM6:J71:PY-IT. The good miscibility between J71 and PM6 enabled the active layer to have well-maintained film morphology without damaging the initial nanoscale network, which resulted in faster charge transfer and suppressed exciton recombination. Thus, a higher PCE of 16.52% was achieved (entry 5 in Table 2), which is signific-

antly higher than the corresponding binary all-PSC based on PM6:PY-IT with PCE of 15.56%.[69]

Reducing cost of the polymer photovoltaic materials is very important for future application of the all-PSCs. Peng *et al*. used smaller fused ring dithienopyrrolo[3,2*b*]benzothiadiazole (BTP) as the central core and synthesized two PSMAs BTP-T2F and BTP-2T2F (Fig. 5).[70] The BTP core significantly lowered the HOMO levels of the polymer acceptors, thus enabled them to pair with polymer donors with low-lying HOMO levels, especially for low-cost PTQ10 polymer donor. In addition, the smaller fused ring unit also simplifies the synthesis route and reduces production costs. Finally, the PCE of 14.32% was achieved in the system of PTQ10:BTP2T2F. When second polymer donor PBDTC-TPD was added into the mixture, the resulting ternary all-PSC realized a PCE of 16.04% (entry 6 in Table 2).

For the ternary all-PSCs based on D:A1:A2 system, Yan *et al*. utilized a B←N-type polymer acceptor BN-T (Fig. 5) in the PM6:PY-IT system as the third component to make ternary all-PSC.[71] The small amount of BN-T prefers to form a more crystalline network with enhanced lamellar and *π*-*π* stacking between PM6 and PY-IT, which facilitates the phase separation of the donor and acceptor. The suitable size crystalline domains provide the resulting ternary all-PSC devices with higher charge generation and more balanced charge transport. In addition, lower nonradiative energy losses in the ternary systems are obtained, which further promote the PCE of the system to over 16% (entry 7 in Table 2). On the basis of PY-IT, Min *et al*. synthesized the PSMA PY2F-T (Fig. 2) by introducing fluorine atoms into the terminal group.[72] When blending PY2F-T polymer acceptor with polymer donor PM6 to fabricate all-PSCs, the PCE of 15.0% was achieved. Afterwards, PYT (Fig. 2) as the third component was introduced into the PM6:PY2F-T system, the PCE of the ternary all-PSC was improved up to 17.2% (entry 8 in Table 2). This is mainly owing to the complementary absorption bands of the acceptors and finely tuned microstructures of the ternary blend by the polymer PYT. Furthermore, the ternary system exhibited better light and thermal stabilities than that of the corresponding binary systems. PYT is one of the most commonly used polymer acceptor, Li *et al*. synthesized the PSMA PYCl-T (Fig. 5) based on the PYT by introducing chlorine substitution on the A-end groups in the A-DA′D-A structure to adjust the aggregation behavior of the polymer.[73] PYCl-T was then employed as the third component into the PM6:PY-IT system to prepare the ternary all-PSC based on PM6:PY-IT:PYCl-T. In the ternary device, PYCl-T played an important role in the formation of homogeneously mixed phase and more ordered molecular aggregation in the blend films. By optimizing the devices, a high PCE of 16.62% was achieved in the PM6:PY-IT:PYCl-T based ternary all-PSC (entry 9 in Table 2). Moreover, Ye *et al*. used the ternary strategy to simultaneously improve device efficiency, mechanical robustness, and stability of all-PSCs.[74] Considering the homologous acceptors PY-IT and PYF-IT (Fig. 5) with the same conjugated backbone can effectively interrupt the crystallinity of indivdual acceptors while adjust their blend morphology. They introducing 50 wt% PYF-IT into the PM6:PY-IT system. Compared with the binary system, the optimal ternary devices exhibit more efficient charge separation and less recombination. The ternary all-PSCs based on PM6:PY-IT:PYF-IT achieved a PCE of 16.6% (entry 10 in Table 2), which is significantly higher than that of the control binary all-PSC with PCE of 15.0%. In addition, the mutual entanglement between polymer acceptor chains makes the ternary all-PSC have more outstanding mechanical properties than the binary blends, which offered the flexible ternary all-PSC with a desirable PCE of 14.5% and maintaining 90% of its initial PCE after bending 1000 cycles.

Recently, several research groups have promoted the efficiency of all-PSCs to even higher levels by ternary strategy. For example, Min *et al*. designed and synthesized two similar PSMAs PY-SSe-V and PY-Cl (Fig. 5) by introducing selenium into the central core and chloride into the end group of the SMA monomers, to modify absorption and crystallinity of the PSMAs.[75] When using PM6 as polymer donor, the PCE of 17.03% for the PM6/PY-SSe-V-based binary device and 16.37% for the PM6/PY-Cl-based binary all-PSC were obtained by the layer-by-layer (LbL) processing technique. It is worth noticing that the LbL-type PM6/PY-SSe-V blend still shows BHJ-like morphology, while the PM6/PY-Cl active layer exhibits a pseudo-planar bilayer architecture. This is mainly because of the PY-Cl exhibiting lower miscibility with PM6 compared with PY-SSe-V. Therefore, taking PY-Cl as the third component will help to inhibit the excessive mixing of PY-SSe-V and PM6 in the LbL-type ternary all-PSCs and could promote the active layer to form an ideal vertical phase separation. This morphological merit is conducive to the enhancement of charge transport properties, and further reduces the non-radiative recombination loss, resulting in a higher PCE of 18.14% (entry 11 in Table 2).[71] Similarly, Sun *et al*.[76] prepared ternary all-PSCs in which PM6:PY-82 was selected as the host blend and PY-DT was employed as a guest component. The polymer PY-DT (Fig. 2) and PY-82 (Fig. 5) are similar in structure but more regular, which can not only ensure the compatibility of materials, but also effectively optimizes the morphology of active layer. As a result, the ternary PM6:PY-82:PY-DT device produces a high PCE of 18.03% (entry 12 in Table 2). In addition, the all-PSCs module (16.5 cm^2) based on this ternary system processed with environmentally friendly solvent (*o*-xylene) has achieved the PCE of 13.84%.[72]

To push all-PSCs toward higher PCE, constructing tandem all-PSCs may be an effective way for surpassing the Shockley-Queisser limit of single-junction solar cells. By pairing the photovoltaic materials with complementary absorption in the front and rear cells, the tandem devices can effectively reduce thermal loss of high energy photons and harvest broader solar spectrum. However, up to now, there are few reports on tandem all-PSCs, which may be due to the slow development of early all-PSCs, thus it is difficult to select two pairs of polymer materials with outstanding efficiency and complementary absorption at the same time.

In 2016, Ma *et al*. first reported a tandem all-PSC using identical sub-cells based on P2F-DO:N2200.[77] As a result, the PCE of 6.70% was achieved, which is 43% higher than the PCE of its single junction cell. In order to utilize absorption complementation strategy to improve device efficiency, then they fabricated the tandem all-PSCs with two different sub-cells. Among them, PTP8:P(NDI2HD-T) (Fig. 6) with good response in the short wavelength region was used as the front cell, while PBFSF:N2200 with strong absorption in the long

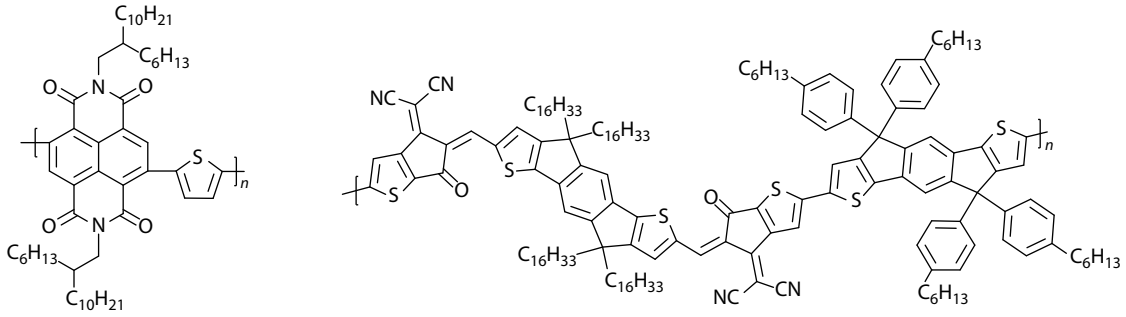

Fig. 6 Molecular structures of the polymer acceptors used in tandem all-PSC.

wavelength region was used as the rear cell. Finally, the tandem all-PSC achieved a higher PCE of 8.3% (entry 13 in Table 2).[78] In 2018, Huang *et al*. used PTzBI-Si as the polymer donor, N2200 as the polymer acceptor, and PNDIT-F3N: PEI/PEDOT as the interconnection layer built a tandem all-PSC.[79] Through fine adjustment of the thickness of the front and rear cells, the device achieved a PCE of 11.2% (entry 14 in Table 2). Furthermore, this tandem all-PSC exhibit improved stability than the single-junction all-PSC, which demonstrated that the tandem all-PSC may be potential candidate to offer a new approach to improve both the PCE and the stability of the PSC devices.

Recently, Li *et al*. fabricated high performance tandem all-PSCs by employing two complementary absorbing PSMAs, a wide bandgap PSMA PIDT (Fig. 6) as the polymer acceptor in the front cell with PM7 as polymer donor and a narrow-bandgap PSMA PY-IT as the polymer acceptor in the rear cell with PM6 as polymer donor.[80] Owing to the complementary absorption spectra of the PSMAs and the polymer donor, the device formed an efficient utilization of sunlight in the 300–900 nm wavelength range. By fine-tuning the active layer thicknesses of the front cell and rear cell, the tandem all-PSC achieved an outstanding PCE of 17.87% (entry 15 in Table 2). Moreover, the tandem all-PSCs show excellent thermal and photo stability compared with their small-molecule counterparts. In the future, the rapid development of PMSAs will provide versatile choice for the polymer acceptors used in the tandem all-PSCs, which will further promote the improvement of the PCE of the tandem all-PSCs.

CONCLUSIONS AND FUTURE OUTLOOK

All-PSCs possess the advantages of mechanical flexibility, morphology-stability, and good film-forming property. Recently, the strategy of the PSMAs and the rapid development of the high performance PSMA polymer acceptors have promoted the PCE of the all-PSCs to the level of 17%–18%, which is close to the efficiency of the SMAs-based PSCs. Therefore, the PSMA-based all-PSCs are promising for the application in future large scale flexible PSCs.

To further boost device performances for the ultimate industrialization, we want to point out the following several issues. (1) The synergistic optimization of SMA building blocks and linking units may provide new opportunities to further improve photovoltaic performance of the PSMAs, by further broadening its absorption, enhancing its electron mobility and optimizing the active layer morphology of the blend of polymer acceptor and polymer donor. (2) It is still a challenge to control the active layer morphology of the blend of polymer acceptor and polymer donor in the all-PSCs. From the thermodynamic point of view, studies on Flory-Huggins type interactions and solubility parameters may give some hints for a better understanding of the phase separation behavior in the active layer, which may instruct the molecular design for the donor and acceptor materials as well as the third component used in the ternary all-PSCs. (3) More diversified polymerization methods for the high performance and low cost PSMAs should be explored to solve the problems of batch difference and low yield of the PSMA polymer acceptors. (4) Stability issue, including the photo-stability, environmental stability and thermal stability, should be deeply studied. (5) Large scale synthesis of the *p*-type conjugated polymer donors and the PSMA polymer acceptors with non-halogenated solvent processing is also very important for future application of the all-PSCs. We believe that the flexible all-PSCs will get our daily life application in near future.

BIOGRAPHIES

Xiao-Jun Li received his Ph.D. degree from Institute of Chemistry, Chinese Academy of Sciences (ICCAS) in 2019 under the supervision of Prof. Yongfang Li. He did postdoctoral research at the Hong Kong University of Science and Technology with Prof. Sir He Yan from 2019 to 2021. Then he joined the Yongfang Li's group in CAS Key Laboratory of Organic Solids, ICCAS, in 2021 and was appointed as an Associate Professor. His main research interests focus on the synthesis and application of organic photovoltaic materials.

Yong-Fang Li is a professor in Institute of Chemistry, Chinese Academy of Sciences (ICCAS) and in Soochow University. He received his Ph.D. degree from department of Chemistry, Fudan University in 1986, then did his postdoctoral research at ICCAS from 1986 to 1988. He became a staff in 1988 and promoted to professor in 1993 in ICCAS. He was elected as a member of Chinese Academy of Sciences in 2013. His present research field is photovoltaic materials and devices for polymer solar cells.

https://doi.org/10.1007/s10118-023-2944-0

NOTES

The authors declare no competing financial interest.

ACKNOWLEDGMENTS

This work was financially supported by the National Natural Science Foundation of China (Nos. 61904181, 51820105003, 52173188 and 21734008) and the Basic and Applied Basic Research Major Program of Guangdong Province (No. 2019B030302007).

REFERENCES

1 Yang, F.; Huang, Y.; Li, Y.; Li, Y. F. Large-area flexible organic solar cells. *npj Flex. Electron.* **2021**, *5*, 30.
2 Li, Y.; Xu, G.; Cui, C.; Li, Y. F. Flexible and semitransparent organic solar cells. *Adv. Energy Mater.* **2018**, *8*, 1701791.
3 Liu, Y.; Liu, B.; Ma, C.; Huang, F.; Feng, G.; Chen, H.; Hou, J.; Yan, L.; Wei, Q.; Luo, Q.; Bao, Q.; Ma, W.; Liu, W.; Li, W.; Wan, X.; Hu, X.; Han, Y.; Li, Y.; Zhou, Y.; Zou, Y.; Chen, Y.; Liu, Y.; Meng, L.; Li, Y.; Chen, Y.; Tang, Z.; Hu, Z.; Zhang, Z; Bo, Z. Recent progress in organic solar cells (Part II Device engineering). *Sci. China Chem.* **2022**, *65*, 1457–1497.
4 Li, Y. F. Molecular design of photovoltaic materials for polymer solar cells: toward suitable electronic energy levels and broad absorption. *Acc. Chem. Res.* **2012**, *45*, 723–733.
5 Xu, G.; Hu, X.; Liao, X.; Chen, Y. Bending-stability interfacial layer as dual electron transport layer for flexible organic photovoltaics. *Chinese J. Polym. Sci.* **2021**, *39*, 1441–1448.
6 Wang, T.; Sun, R.; Yang, X. R.; Wu, Y.; Wang, W.; Li, Q.; Zhang, C. F.; Min, J. A near-infrared polymer acceptor enables over 15% efficiency for all-polymer solar cells. *Chinese J. Polym. Sci.* **2022**, *40*, 877–888.
7 Yu, G.; Gao, J.; Hummelen, J.; Wudl, F.; Heeger, A. Polymer photovoltaic cells: enhanced efficiencies via a network of internal donor-acceptor heterojunctions. *Science* **1995**, *270*, 1789–1791.
8 Yu, G.; Heeger, A. Charge separation and photovoltaic conversion in polymer composites with internal donor/acceptor heterojunctions. *J. Appl. Phys.* **1995**, *78*, 4510–4515.
9 He, Y.; Li, Y. F. Fullerene derivative acceptors for high performance polymer solar cells. *Phys. Chem. Chem. Phys.* **2011**, *13*, 1970–1983.
10 Wei, Q.; Liu, W.; Leclerc, M.; Yuan, J.; Chen, H.; Zou, Y. A-DA'D-A non-fullerene acceptors for high-performance organic solar cells. *Sci. China Chem.* **2020**, *63*, 1352–1366.
11 Zhang, M.; Bai, Y.; Sun, C.; Xue, L.; Wang, H.; Zhang, Z. Perylene-diimide derived organic photovoltaic materials. *Sci. China Chem.* **2022**, *65*, 462–485.
12 Shi, Y.; Wang, Y.; Guo, X. Recent progress of imide-functionalized N-type polymer semiconductors. *Acta Polymerica Sinica* (in Chinese) **2019**, *50*, 873–889.
13 Lin, Y.; Wang, J.; Zhang, Z.; Bai, H.; Li, Y.; Zhu, D.; Zhan, X. An electron acceptor challenging fullerenes for efficient polymer solar cells. *Adv. Mater.* **2015**, *27*, 1170–1174.
14 Lin, Y.; He, Q.; Zhao, F.; Huo, L.; Mai, J.; Lu, X.; Su, C.; Li, T.; Wang, J.; Zhu, J.; Sun, Y.; Wang, C.; Zhan, X. A facile planar fused-ring electron acceptor for as-cast polymer solar cells with 8.71% efficiency. *J. Am. Chem. Soc.* **2016**, *138*, 2973–2976.
15 Zhang, Z.; Yang, Y.; Yao, J.; Xue, L.; Chen, S.; Li, X.; Morrison, W.; Yang, C.; Li, Y. F. Constructing a strongly absorbing low-bandgap polymer acceptor for high-performance all-polymer solar cells. *Angew. Chem. Int. Ed.* **2017**, *56*, 13503–13507.
16 Zhang, Z.; Li, Y. F. Polymerized small-molecule acceptors for high-performance all-polymer solar cells. *Angew. Chem. Int. Ed.* **2021**, *60*, 4422–4433.
17 Sun, G.; Jiang, X.; Li, X. J; Meng, L.; Zhang, J.; Qin, S.; Kong, X.; Li, J.; Xin, J.; Ma, W.; Li, Y. F. High performance polymerized small molecule acceptor by synergistic optimization on pi-bridge linker and side chain. *Nat. Commun.* **2022**, *13*, 5267.
18 Wang, J.; Cui, Y.; Xu, Y.; Xian, K.; Bi, P.; Chen, Z.; Zhou, K.; Ma, L.; Zhang, T.; Yang, Y.; Zu, Y.; Yao, H.; Hao, X.; Ye, L.; Hou, J. A new polymer donor enables binary all-polymer organic photovoltaic cells with 18% efficiency and excellent mechanical robustness. *Adv. Mater.* **2022**, *34*, 2205009.
19 Zhan, X.; Tan, Z. A.; Domercq, B.; An, Z.; Zhang, X.; Barlow, S.; Li, Y.; Zhu, D.; Kippelen, B.; Marder, S. R. A high-mobility electron-transport polymer with broad absorption and its use in field-effect transistors and all-polymer solar cells. *J. Am. Chem. Soc.* **2007**, *129*, 7246–7247.
20 Guo, X.; Watson, M. Conjugated polymers from naphthalene bisimide. *Org. Lett.* **2008**, *10*, 5333–5336.
21 Yan, H.; Chen, Z.; Zheng, Y.; Newman, C.; Quinn, J.; Dotz, F.; Kastler, M.; Facchetti, A. A high-mobility electron-transporting polymer for printed transistors. *Nature* **2009**, *457*, 679–686.
22 Kang, H.; Uddin, M.; Lee, C.; Kim, K.; Thanh L.; Lee, W.; Li, Y.; Wang, C.; Woo, H.; Kim, B. Determining the role of polymer molecular weight for high-performance all-polymer solar cells: its effect on polymer aggregation and phase separation. *J. Am. Chem. Soc.* **2015**, *137*, 2359–2365.
23 Zhang, Z.; Bai, Y.; Li, Y. F. Benzotriazole based 2D-conjugated polymer donors for high performance polymer solar cells. *Chinese J. Polym. Sci.* **2021**, *39*, 1–13.
24 Gao, L.; Zhang, Z.; Xue, L.; Min, J.; Zhang, J.; Wei, Z.; Li, Y. All-polymer solar cells based on absorption-complementary polymer donor and acceptor with high power conversion efficiency of 8.27%. *Adv. Mater.* **2016**, *28*, 1884–1890.
25 Li, Z.; Zhong, W.; Ying, L.; Liu, F.; Li, N.; Huang, F.; Cao, Y. Morphology optimization *via* molecular weight tuning of donor polymer enables all-polymer solar cells with simultaneously improved performance and stability. *Nano Energy* **2019**, *64*, 103931.
26 Li, W.; Roelofs, W.; Turbiez, M.; Wienk, M.; Janssen, R. Polymer solar cells with diketopyrrolopyrrole conjugated polymers as the electron donor and electron acceptor. *Adv. Mater.* **2014**, *26*, 3304–3309.
27 Sun, H.; Tang, Y.; Koh, C.; Ling, S.; Wang, R.; Yang, K.; Yu, J.; Shi, Y.; Wang, Y.; Woo, H.; Guo, X. High-performance all-polymer solar cells enabled by an N-type polymer based on a fluorinated imide-functionalized arene. *Adv. Mater.* **2019**, *31*, 1807220.
28 Zhao, R.; Liu, J.; Wang, L. Polymer acceptors containing B←N units for organic photovoltaics. *Acc. Chem. Res.* **2020**, *53*, 1557–1567.
29 Zhang, Y. Z.; Wang, N.; Wang, Y. H.; Miao, J. H.; Liu, J.; Wang, L. X. 15% Efficiency all-polymer solar cells based on a polymer acceptor containing B←N unit. *Chinese J. Polym. Sci.* **2022**, *40*, 989–995.
30 Meng, Y.; Wu, J.; Guo, X.; Su, W.; Zhu, L.; Fang, J.; Zhang, Z.; Liu, F.; Zhang, M.; Russell, T.; Li, Y. F. 11.2% Efficiency all-polymer solar cells with high open-circuit voltage. *Sci. China Chem.* **2019**, *62*, 845–850.
31 Yao, H.; Ma, L.; Yu, H.; Yu, J.; Chow, P.; Xue, W.; Zou, X.; Chen, Y.; Liang, J.; Arunagiri, L.; Gao, F.; Sun, H.; Zhang, G.; Ma, W.; Yan, H. All-polymer solar cells with over 12% efficiency and a small voltage loss enabled by a polymer acceptor based on an extended fused ring core. *Adv. Energy Mater.* **2020**, *10*, 2001408.
32 Yuan, J.; Zhang, Y.; Zhou, L.; Zhang, G.; Yip, H.; Lau, T.; Lu, X.; Zhu, C.; Peng, H.; Johnson, P.; Leclerc, M.; Cao, Y.; Ulanski, J.; Li, Y.; Zou, Y. Single-junction organic solar cell with over 15% efficiency

using fused-ring acceptor with electron-deficient core. *Joule* **2019**, *3*, 1140–1151.
33 Jia, T.; Zhang, J.; Zhong, W.; Liang, Y.; Zhang, K.; Dong, S.; Ying, L.; Liu, F.; Wang, X.; Huang, F.; Cao, Y. 14.4% Efficiency all-polymer solar cell with broad absorption and low energy loss enabled by a novel polymer acceptor. *Nano Energy* **2020**, *72*, 104718.
34 Wang, W.; Wu, Q.; Sun, R.; Guo, J.; Wu, Y.; Shi, M.; Yang, W.; Li, H.; Min, J. Controlling molecular mass of low-band-gap polymer acceptors for high-performance all-polymer solar cells. *Joule* **2020**, *4*, 1070–1086.
35 Fan, Q.; Fu, H.; Wu, Q.; Wu, Z.; Lin, F.; Zhu, Z.; Min, J.; Woo, H.; Jen, A. Multi-selenophene-containing narrow bandgap polymer acceptors for all-polymer solar cells with over 15% efficiency and high reproducibility. *Angew. Chem. Int. Ed.* **2021**, *60*, 15935–15943.
36 Fu, H.; Fan, Q.; Gao, W.; Oh, J.; Li, Y.; Lin, F.; Qi, F.; Yang, C.; Marks, T.; Jen, A. 16.3% Efficiency binary all-polymer solar cells enabled by a novel polymer acceptor with an asymmetrical selenophene-fused backbone. *Sci. China Chem.* **2022**, *65*, 309–317.
37 Fu, H.; Li, Y.; Yu, J.; Wu, Z.; Fan, Q.; Lin, F.; Woo, H.; Gao, F.; Zhu, Z.; Jen, A. High efficiency (15.8%) all-polymer solar cells enabled by a regioregular narrow bandgap polymer acceptor. *J. Am. Chem. Soc.* **2021**, *143*, 2665–2670.
38 Du, J.; Hu, K.; Zhang, J.; Meng, L.; Yue, J.; Angunawela, I.; Yan, H.; Qin, S.; Kong, X.; Zhang, Z.; Guan, B.; Ade, H.; Li, Y. Polymerized small molecular acceptor based all-polymer solar cells with an efficiency of 16.16% *via* tuning polymer blend morphology by molecular design. *Nat. Commun.* **2021**, *12*, 5264.
39 Li, Y.; Song, J.; Dong, Y.; Jin, H.; Xin, J.; Wang, S.; Ca, Y.; Jiang, L.; Ma, W.; Tang, Z.; Sun, Y. Polymerized small molecular acceptor with branched side chains for all polymer solar cells with efficiency over 16.7%. *Adv. Mater.* **2022**, *34*, 2110155.
40 Luo, Z.; Liu, T.; Ma, R.; Xiao, Y.; Zhan, L.; Zhang, G.; Sun, H.; Ni, F.; Chai, G.; Wang, J.; Zhong, C.; Zou, Y.; Guo, X.; Lu, X.; Chen, H.; Yan, H.; Yang, C. Precisely controlling the position of bromine on the end group enables well-regular polymer acceptors for all-polymer solar cells with efficiencies over 15%. *Adv. Mater.* **2020**, *32*, 2005942.
41 Peng, F.; An, K.; Zhong, W.; Li, Z.; Ying, L.; Li, N.; Huang, Z.; Zhu, C.; Fan, B.; Huang, F.; Cao, Y. A universal fluorinated polymer acceptor enables all-polymer solar cells with >15% efficiency. *ACS Energy Lett.* **2020**, *5*, 3702–3707.
42 Yu, H.; Luo, S.; Sun, R.; Angunawela, I.; Qi, Z.; Peng, Z.; Zhou, W.; Han, H.; Wei, R.; Pan, M.; Cheung, A.; Zhao, D.; Zhang, J.; Ade, H.; Min, J.; Yan, H. A difluoro-monobromo end group enables high-performance polymer acceptor and efficient all-polymer solar cells processable with green solvent under ambient condition. *Adv. Funct. Mater.* **2021**, *31*, 2100791.
43 Li, Y.; Jia, Z.; Zhang, Q.; Wu, Z.; Qin, H.; Yang, J.; Wen, S.; Woo, H.; Ma, W.; Yang, R.; Yuan, J. Toward efficient all-polymer solar cells *via* halogenation on polymer acceptors. *ACS Appl. Mater. Interfaces* **2020**, *12*, 33028–33038.
44 Wang, H.; Chen, H.; Xie, W.; Lai, H.; Zhao, T.; Zhu, Y.; Chen, L.; Ke, C.; Zheng, N.; He, F. Configurational isomers induced significant difference in all-polymer solar cells. *Adv. Funct. Mater.* **2021**, *31*, 2100877.
45 Yu, H.; Wang, Y.; Kim, H.; Wu, X.; Li, Y.; Yao, Z.; Pan, M.; Zou, X.; Zhang, J.; Chen, S.; Zhao, D.; Huang, F.; Lu, X.; Zhu, Z.; Yan, H. A vinylene-linker-based polymer acceptor featuring a coplanar and rigid molecular conformation enables high-performance all-polymer solar cells with over 17% efficiency. *Adv. Mater.* **2022**, *34*, 2200361.
46 Liu, F.; Sun, R.; Wang, C. Y.; Zhou, L.; Su, W. L.; Yue, Q. H.; Sun, S.; Liu, W. Y.; Fan, H. J.; Zhang, W. K.; Guo, Y. L.; Feng, L. H.; Zhu, X. Z. Planarized polymer acceptor featuring high electron mobility for efficient all-polymer solar cells. *Chinese J. Polym. Sci.* **2022**, *40*, 968–978.
47 Yao, H.; Bai, F.; Hu, H.; Arunagiri, L.; Zhang, J.; Chen, Y.; Yu, H.; Chen, S.; Liu, T.; Lai, J.; Zou, Y.; Ade, H.; Yan, H. Efficient all-polymer solar cells based on a new polymer acceptor achieving 10.3% power conversion efficiency. *ACS Energy Lett.* **2019**, *4*, 417–422.
48 Fan, Q.; An, Q.; Lin, Y.; Xia, Y.; Li, Q.; Zhang, M.; Su, W.; Peng, W.; Zhang, C.; Liu, F.; Hou, L.; Zhu, W.; Yu, D.; Xiao, M.; Moons, E.; Zhang, F.; Anthopoulos, T.; Inganas, O.; Wang, E. Over 14% efficiency all-polymer solar cells enabled by a low bandgap polymer acceptor with low energy loss and efficient charge separation. *Energy Environ. Sci.* **2020**, *13*, 5017–5027.
49 Sun, H.; Yu, H.; Shi, Y.; Yu, J.; Peng, Z.; Zhang, X.; Liu, B.; Wang, J.; Singh, R.; Lee, J.; Li, Y.; Wei, Z.; Liao, Q.; Kan, Z.; Ye, L.; Yan, H.; Gao, F.; Guo, X. A narrow-bandgap N-type polymer with an acceptor-acceptor backbone enabling efficient all-polymer solar cells. *Adv. Mater.* **2020**, *32*, 2004183.
50 Zhou, L.; Xia, X.; Meng, L.; Zhang, J.; Lu, X.; Li, Y. Introducing electron-withdrawing linking units and thiophene π-bridges into polymerized small molecule acceptors for high-efficiency all-polymer solar cells. *Chem. Mater.* **2021**, *33*, 8212–8222.
51 Fan, Q.; Ma, R.; Liu, T.; Yu, J.; Xiao, Y.; Su, W.; Cai, G.; Li, Y.; Peng, W.; Guo, T.; Luo, Z.; Sun, H.; Hou, L.; Zhu, W.; Lu, X.; Gao, F.; Moons, E.; Yu, D.; Yan, H.; Wang, E. High-performance all-polymer solar cells enabled by a novel low bandgap non-fully conjugated polymer acceptor. *Sci. China Chem.* **2021**, *64*, 1380–1388.
52 Liu, W.; Yuan, J.; Zhu, C.; Wei, Q.; Liang, S.; Zhang, H.; Zheng, G.; Hu, Y.; Meng, L.; Gao, F.; Li, Y.; Zou, Y. A-π-A structured non-fullerene acceptors for stable organic solar cells with efficiency over 17%. *Sci. China Chem.* **2022**, *65*, 1374–1382.
53 Benten, H.; Nishida, T.; Mori, D.; Xu, H.; Ohkita, H.; Ito, S. High-performance ternary blend all-polymer solar cells with complementary absorption bands from visible to near-infrared wavelengths. *Energy Environ. Sci.* **2016**, *9*, 135–140.
54 Su, W.; Fan, Q.; Guo, X.; Guo, B.; Li, W.; Zhang, Y.; Zhang, M.; Li, Y. Efficient ternary blend all-polymer solar cells with a polythiophene derivative as a hole-cascade material. *J. Mater. Chem. A* **2016**, *4*, 14752–14760.
55 Liu, J.; Tang, B.; Liang, Q.; Han, Y.; Xie, Z.; Liu, J. Dual Förster resonance energy transfer and morphology control to boost the power conversion efficiency of all-polymer OPVs. *RSC Adv.* **2017**, *7*, 13289–13298.
56 Li, Z.; Xu, X.; Zhang, W.; Meng, X.; Genene, Z.; Ma, W.; Mammo, W.; Yartsev, A.; Andersson, M.; Janssen, R.; Wang, E. 9.0% Power conversion efficiency from ternary all-polymer solar cells. *Energy Environ. Sci.* **2017**, *10*, 2212–2221.
57 Li, Z.; Fan, B.; He, B.; Ying, L.; Zhong, W.; Liu, F.; Huang, F.; Cao, Y. Side-chain modification of polyethylene glycol on conjugated polymers for ternary blend all-polymer solar cells with efficiency up to 9.27%. *Sci. China Chem.* **2018**, *61*, 427–436.
58 Li, Z.; Ying, L.; Xie, R.; Zhu, P.; Li, N.; Zhong, W.; Huang, F.; Cao, Y. Designing ternary blend all-polymer solar cells with an efficiency of over 10% and a fill factor of 78%. *Nano Energy* **2018**, *51*, 434–441.
59 Chen, H.; Guo, Y.; Chao, P.; Liu, L.; Chen, W.; Zhao, D.; He, F. A chlorinated polymer promoted analogue co-donors for efficient ternary all-polymer solar cells. *Sci. China Chem.* **2019**, *62*, 238–244.
60 Liu, S.; Chen, D.; Zhou, W.; Yu, Z.; Chen, L.; Liu, F.; Chen, Y. Vertical distribution to optimize active layer morphology for efficient all-polymer solar cells by J71 as a compatibilizer. *Macromolecules* **2019**, *52*, 4359–4369.
61 Zhang, Q.; Chen, Z.; Ma, W.; Xie, Z.; Liu, J.; Yu, X.; Han, Y. Efficient nonhalogenated solvent-processed ternary all-polymer solar

cells with a favorable morphology enabled by two well-compatible donors. *ACS Appl. Mater. Interfaces* **2019**, *11*, 32200–32208.
62 Zhou, K.; Zhou, X.; Xu, X.; Musumeci, C.; Wang, C.; Xu, W.; Meng, X.; Ma, W.; Inganas, O. *π-π* Stacking distance and phase separation controlled efficiency in stable all-polymer solar cells. *Polymers* **2019**, *11*, 1665.
63 Liu, X.; Zhang, C.; Pang, S.; Li, N.; Brabec, C.; Duan, C.; Huang, F.; Cao, Y. Ternary all-polymer solar cells with 8.5% power conversion efficiency and excellent thermal stability. *Front. Chem.* **2020**, *8*, 302.
64 Wang, K.; Dong, S.; Chen, X.; Zhou, P.; Zhang, K.; Huang, J.; Wang, M. Improving the all-polymer solar cell performance by adding a narrow bandgap polymer as the second donor. *RSC Adv.* **2020**, *10*, 38344–38350.
65 Xu, X.; Feng, K.; Yu, L.; Yan, H.; Li, R.; Peng, Q. Highly efficient all-polymer solar cells enabled by P-doping of the polymer donor. *ACS Energy Lett.* **2020**, *5*, 2434–2443.
66 Hu, K.; Du, J.; Sun, C.; Zhu, C.; Zhang, J.; Yao, J.; Zhang, Z.; Wan, Y.; Zhang, Z.; Meng, L.; Li, Y. F. Ternary all-polymer solar cells with two synergetic donors enable efficiency over 14.5%. *Energy Fuel.* **2021**, *35*, 19045–19054.
67 Zhang, W.; Sun, C.; Angunawela, I.; Meng, L.; Qin, S.; Zhou, L.; Li, S.; Zhuo, H.; Yang, G.; Zhang, Z.; Ade, H.; Li, Y. 16.52% Efficiency all-polymer solar cells with high tolerance of the photoactive layer thickness. *Adv. Mater.* **2022**, *34*, 2108749.
68 An, K.; Peng, F.; Zhong, W.; Deng, W.; Zhang, D.; Ying, L.; Wu, H.; Huang, F.; Cao, Y. Improving photovoltaic parameters of all-polymer solar cells through integrating two polymeric donors. *Sci. China Chem.* **2021**, *64*, 2010–2016.
69 Ma, R.; Zhou, K.; Sun, Y.; Liu, T.; Kan, Y.; Xiao, Y.; Dela, T.; Li, Y.; Zou, X.; Xing, Z.; Luo, Z.; Wong, K.; Lu, X.; Ye, L.; Yan, H.; Gao, K. Achieving high efficiency and well-kept ductility in ternary all-polymer organic photovoltaic blends thanks to two well miscible donors. *Matter* **2022**, *5*, 725–734.
70 Liao, C.; Gong, Y.; Xu, X.; Yu, L.; Li, R.; Peng, Q. Cost-efficiency balanced polymer acceptors based on lowly fused dithienopyrrolo[3, 2*b*]benzothiadiazole for 16.04% efficiency all-polymer solar cells. *Chem. Eng. J.* **2022**, *435*, 134862.
71 Liu, T.; Yang, T.; Ma, R.; Zhan, L.; Luo, Z.; Zhang, G.; Li, Y.; Gao, K.; Xiao, Y.; Yu, J.; Zou, X.; Sun, H.; Zhang, M.; Dela, T.; Xing, Z.; Liu, H.; Li, X.; Li, G.; Huang, J.; Duan, C.; Wong, K.; Lu, X.; Guo, X.; Gao, F.; Chen, H.; Huang, F.; Li, Y.; Li, Y.; Cao, Y.; Tang, B.; Yan, H. 16% Efficiency all-polymer organic solar cells enabled by a finely tuned morphology *via* the design of ternary blend. *Joule* **2021**, *5*, 914–930.
72 Sun, R.; Wang, W.; Yu, H.; Chen, Z.; Xia, X.; Shen, H.; Guo, J.; Shi, M.; Zheng, Y.; Wu, Y.; Yang, W.; Wang, T.; Wu, Q.; Yang, Y.; Lu, X.; Xia, J.; Brabec, C.; Yan, H.; Li, Y.; Min, J. Achieving over 17% efficiency of ternary all-polymer solar cells with two well-compatible polymer acceptors. *Joule* **2021**, *5*, 1548–1565.
73 Hu, K.; Du, J.; Zhu, C.; Lai, W.; Li, J.; Xin, J.; Ma, W.; Zhang, Z.; Zhang, J.; Meng, L.; Li, Y. F. Chlorinated polymerized small molecule acceptor enabling ternary all-polymer solar cells with over 16.6% efficiency. *Sci. China Chem.* **2022**, *65*, 954–963.
74 Xian, K.; Zhou, K.; Li, M.; Liu, J.; Zhang, Y.; Zhang, T.; Cui, Y.; Zhao, W.; Yang, C.; Hou, J.; Geng, Y.; Ye, L. Simultaneous optimization of efficiency, stretchability, and stability in all-polymer solar cells *via* aggregation control. *Chin. J. Chem.* **2023**, *41*, 159–166.
75 Yang, X.; Sun, R.; Wang, Y.; Chen, M.; Xia, X.; Lu, X.; Lu, G.; Min, J. Ternary all-polymer solar cells with efficiency up to 18.14% employing a two-step sequential deposition. *Adv. Mater.* **2023**, *35*, 2209350.
76 Cai, Y.; Xie, C.; Li, Q.; Liu, C.; Gao, J.; Jee, M.; Qiao, J.; Li, Y.; Song, J.; Hao, X.; Woo, H.; Tang, Z.; Zhou, Y.; Zhang, C.; Huang, H.; Sun, Y. Improved molecular ordering in a ternary blend enables all-polymer solar cells over 18% efficiency. *Adv. Mater.* **2022**, 2208165.
77 Yuan, J.; Gu, J.; Shi, G.; Sun, J.; Wang, H.; Ma, W. High efficiency all-polymer tandem solar cells. *Sci. Rep.* **2016**, *6*, 26459.
78 Yuan, J.; Ford, M.; Xu, Y.; Zhang, Y.; Bazan, G.; Ma, W. Improved tandem all-polymer solar cells performance by using spectrally matched subcells. *Adv. Energy Mater.* **2018**, *8*, 1703291.
79 Zhang, K.; Xia, R.; Fan, B.; Liu, X.; Wang, Z.; Dong, S.; Yip, H.; Ying, L.; Huang, F.; Cao, Y. 11.2% All-polymer tandem solar cells with simultaneously improved efficiency and stability. *Adv. Mater.* **2018**, *30*, 1803166.
80 Ma, Q.; Jia, Z.; Meng, L.; Yang, H.; Zhang, J.; Lai, W.; Guo, J.; Jiang, X.; Cui, C.; Li, Y. F. 17.87% Efficiency all-polymer tandem solar cell enabled by complementary absorbing polymer acceptors. *Adv. Funct. Mater.* **2023**, *33*, 2210733.

https://doi.org/10.1007/s10118-023-2944-0